

# Stochastic Modeling and Control for Tracking the Periodic Movement of Marine Animals via AUVs

Kevin D. Smith<sup>1</sup>, Shih-Chieh Hsiung<sup>2</sup>, Connor White<sup>3</sup>  
Christopher G. Lowe<sup>4</sup> and Christopher M. Clark<sup>5</sup>

**Abstract**—This paper presents a graph-based model of periodic migrations of tagged fish populations and two multi-AUV stochastic controllers developed to track these fish from the model. The model presented in this paper characterizes patterns in the historical movement of tagged fish and is used to develop stochastic tracking by a “model based control” and a “feedback control”. These two controllers permit swarms of AUVs to track the transition probabilities of the tagged population between vertices of the model. To validate these controllers, a periodic model is developed for a simulated population based on three months of geolocation data from a kelp bass (*Paralabrax clathratus*), and AUV teams utilizing both controllers are simulated in tracking this population. Results show the viability of stochastic controls for multi-AUV tracking of populations whose behavior is well-approximated by the graph-based model. Preliminary trials with physical AUV systems indicate the plausibility of hardware implementation.

## I. INTRODUCTION

The study of marine environments provides the knowledge necessary for monitoring and sustaining our planet. Understanding fish movement patterns with respect to their habitats, through observation and modeling can provide us with essential information for making decisions that affect our environment, health, finances, and safety.

This paper establishes graph-based, stochastic models of such movement patterns, as well as stochastic motion planning controls for Autonomous Underwater Vehicles (AUVs) that leverage these models to enable autonomous tracking of populations. Specifically, the work focuses on the stochastic modeling and AUV tracking of periodic fish movement patterns, particularly diel migrations. Such periodic migratory behavior including diel, lunar and seasonal migrations can be found in a large number of marine fishes [1], [2], [3], [4].

A data set of time-stamped geolocations of kelp bass (*Paralabrax clathratus*) collected at Big Fisherman’s Cove, Santa Catalina Island, California, motivates this work. In 2010, three individuals tagged with acoustic transmitters were tracked by a static acoustic array from January through

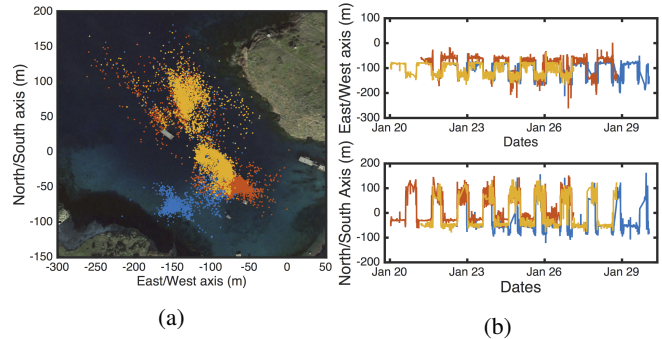


Fig. 1: A three-month track of three tagged fish motivated this work. (a) The aggregated detections showed a high degree of clustering. (b) Furthermore, migrations between these clusters were periodic.

March, yielding the scatterplot of data in Fig. 1a. This plot reveals several clusters of frequented locations, permitting discretization of the tracking space. Furthermore, as shown in Fig. 1b, the bass exhibited highly periodic behavior which is amenable to stochastic modeling.

The contributions of this work include the following:

- Graph-based modeling of (periodic) migrations
- Two stochastic AUV control systems that enable tracking of graph vertices: 1) a model-based control, and 2) a nonlinear feedback control, with proof of convergence
- Simulated verification of the control systems
- Implementation of control systems on a physical AUV to demonstrate hardware implementation plausibility

Our general approach to stochastic tracking consists of two broad steps. First, fish movements are modeled as transitions between vertices on a graph, using historical tracks. These measurements are used to generate a transition model, which predicts future distributions of fish population density over the graph. This modeling can occur online in real-time, or offline before tracking occurs. Section III provides a mathematical derivation of this graph-based modeling.

Second, a control system distributes AUVs over the graph in real-time to minimize the difference between AUV and fish population densities. Section IV describes two possible control systems: a model-based control, tracking historical transition probabilities; and a feedback control, which monitors real-time detections and distributes AUVs accordingly. Section V validates these controls in simulation, and Section VI discusses preliminary experiments implementing such systems on physical AUVs.

<sup>1</sup>Kevin D. Smith is with the Department of Physics, Harvey Mudd College, Claremont, CA 91711 ksmith@g.hmc.edu

<sup>2</sup>Shih-Chieh Hsiung is with the Department of Computer Science, Harvey Mudd College, Claremont, CA 91711 shsiung@g.hmc.edu

<sup>3</sup>Connor White is with the Department of Biological Sciences, California State University Long Beach, Long Beach, CA 90840 connor.white@student.csulb.edu

<sup>4</sup>Christopher G. Lowe is with the Department of Biological Sciences, California State University Long Beach, Long Beach, CA 90840 clowe@csulb.edu

<sup>5</sup>Christopher M. Clark is with the Department of Engineering, Harvey Mudd College, Claremont, CA 91711 clark@hmc.edu

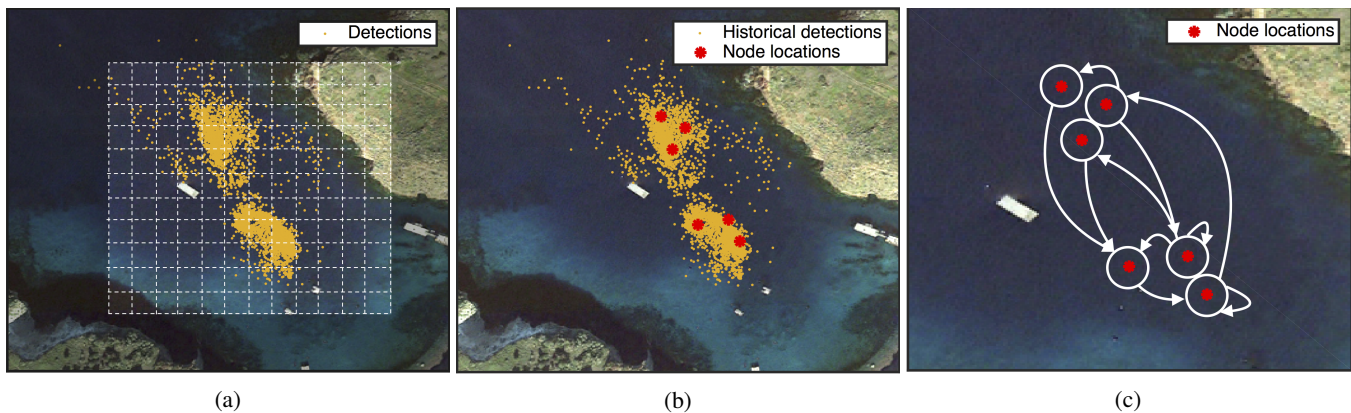


Fig. 2: To create a transition model, the area of interest is first discretized to vertices, by gridding (a) or other processes like k-means clustering (b). Historical data then informs the choice of time-dependent transition probabilities between vertices (c).

## II. BACKGROUND

Patterns of movement of marine animals change with environmental conditions, species interactions, and social context. For example, water temperature can affect animals aggregation locations, and rapid drops in barometric pressure associated with storm fronts trigger mass migrations from shallow water to deeper habitats [5], [6]. Investigation of periodic migratory paths is particularly important in understanding both environmental factors and migratory behavior of marine animals, as periodic changes in environmental factors drive the movement of several species of marine animals [7], [8], [9]. Such periodic patterns of movement can also inform tracking.

Tracking marine animals historically includes tagging individuals with acoustic transmitters and using a receiver-array to detect pings from the tags [10], [11]. Active tracking of marine movement patterns has traditionally required mounting a directional hydrophone on a boat and following tagged animals to acquire geositions for up to 72 hours at a time [12]. Advancements in the last few decades have introduced automated methods of tracking humans and other objects [13], [14], [15], [16]. More recently, methods of tracking marine animals with robotic visual and acoustic systems are beginning to develop [17], [18], [19], [20], [21].

Unlike the previous work [22], [23], [24] relating to autonomous tracking of tagged individuals with AUVs, this work presents stochastic control systems that utilize either historical or real-time detections, capable of handling multiple AUVs and tagged individuals. These control systems allocate robots according to changing target densities. Similar work [25], [26], [27] exists on ground-based robots tracking target distributions, where swarms of robots were deployed stochastically for specific tasks such as site visits.

## III. TRANSITION MODELING

### A. Discretization

The tracking problem is simplified by partitioning the space of possible fish locations into a set  $V$  of discrete

vertices. These vertices may be chosen by any process, such as gridding or k-means clustering. Fig. 2a illustrates a uniform grid discretization over the motivating data set while Fig. 2b illustrates a k-means clustered data set with  $k=6$ . To note, the vertices used in this work were stationary, but this is not a requirement.

Then, for a tracked population of  $M$  fish, the vertex occupied by a particular fish  $s \in \{1, 2, \dots, M\}$  at time  $k$  is denoted  $v_{f,s}[k] \in \{1, 2, \dots, |V|\}$ . The fish population density of a particular vertex  $i \in V$  is defined as:

$$p_{f,i}[k] = \frac{1}{M} |\{s \in \{1, 2, \dots, M\} \mid v_{f,s}[k] = i\}| \quad (1)$$

Since

$$\sum_{i \in V} p_{f,i}[k] = 1 \quad (2)$$

the vector of fish population densities  $\mathbf{p}_f[k] = (p_{f,1}[k] \ p_{f,2}[k] \ \dots \ p_{f,|V|}[k])^T$  is a stochastic vector.

### B. Transition Modeling

Given a set of vertices  $V$ , movements of fish are then modeled as transitions between the vertices, akin to following the edges of a graph  $G(V, E)$  formed by the vertices and a set of edges  $E$  between adjacent vertices.

Since many species of fish show periodic patterns of movement, analysis of previous fish locations may predict future distributions of the fish population over the location graph. These predictions take the form of a *transition model*, a  $|V| \times |V|$  left stochastic transition matrix  $\mathbf{T}_f[k]$ , in which the  $i, j$ -th entry indicates the probability of a fish at vertex  $j$  transitioning to vertex  $i$  at time  $k$ . Hence the dynamics can be written as:

$$\mathbf{p}_f[k+1] = \mathbf{T}_f[k] \mathbf{p}_f[k] \quad (3)$$

A transition matrix can be constructed by choosing transition probabilities that direct AUVs toward the populated vertices at each time.

A positive-valued kernel function  $K_h$ , such as a Gaussian curve with smoothing parameter  $h$

$$K_h(x) = \exp\left(-\frac{x^2}{2h^2}\right) \quad (4)$$

is added to the transition probability  $T_{ij}[k]$  at each time any fish is located at vertex  $i$ . More formally, if  $X_{i,s} = \{k_0 \mid v_{f,s}[k_0] = i\}$  is the set of times at which a fish  $s$  is located at vertex  $i$ , then

$$T_{ij}[k] = \frac{1}{C_j} \sum_{s=1}^M \sum_{k_0 \in X_{i,s}} K_h(k - k_0) \quad (5)$$

where  $C_j$  is a normalization factor

$$C_j = \sum_{j=1}^{|V|} T_{ij}[k_0] \quad (6)$$

to enforce that the transition matrix is left stochastic.

The use of a kernel function serves to smooth the transition probabilities and avoid over-fitting. Sharper kernel functions will result in a transition matrix whose expected fish population densities are closer to those of the population being modeled, at the expense of sharper and less-periodic transition probabilities.

From some initial population density  $\mathbf{p}_f[0]$ , the transition model makes a prediction for subsequent population densities by (3). These predictions  $\mathbf{p}_{\text{model}}$  can be compared with the population density  $\mathbf{p}_f[k]$  to be modeled, with discrepancies between the densities quantified by the error term

$$e_{\mathbf{p}} = \sqrt{\frac{1}{2} (\mathbf{p}_{\text{fish}} - \mathbf{p}_{\text{model}}) \cdot (\mathbf{p}_{\text{fish}} - \mathbf{p}_{\text{model}})} \quad (7)$$

that ranges from zero (for identical densities) to one (where all fish in one vector are located at vertex  $i$ , all fish in the other are at vertex  $j$ , and  $i \neq j$ ).

To test this model, the location of one of the kelp bass mentioned in the introduction was estimated at two-minute intervals by linear interpolation over a course of ten days, and it was discretized into six vertices, chosen by k-means clustering (see Fig. 2 (b)). A transition model was fit to the resulting sequence of vertices by the above method, with a Gaussian kernel and smoothing parameter  $h$  of 2 minutes. The population density predictions of this model had an average error of 0.09 over the entire ten day period.

#### IV. CONTROL SYSTEMS

Once a transition model has been constructed, a team of  $N$  AUVs can utilize the model to track the population. Similar to the fish, the AUVs can be distributed across  $V$ , and the location of a particular AUV  $r \in \{1, 2, \dots, N\}$  is denoted  $v_{\text{AUV},r}$ . The AUV population density of a particular vertex  $i \in V$  is

$$p_{\text{AUV},i}[k] = \frac{1}{N} |\{r \in \{1, 2, \dots, N\} \mid v_{\text{AUV},r}[k] = i\}| \quad (8)$$

so that

$$\sum_{i \in V} p_{\text{AUV},i}[k] = 1 \quad (9)$$

Where as the fish use linear dynamics based on the modeled transition matrix  $T_f[k]$ , the AUV population density vector  $\mathbf{p}_{\text{AUV}}[k]$  is updated according to the transition matrix  $T_{\text{AUV}}[k]$ .

$$\mathbf{p}_{\text{AUV}}[k+1] = \mathbf{T}_{\text{AUV}}[k] \mathbf{p}_{\text{AUV}}[k] \quad (10)$$

The goal of the control system, is to construct  $\mathbf{T}_{\text{AUV}}[k]$  at each time step so as to minimize the difference between each vertex's fish population density  $\mathbf{p}_f[k]$  and its AUV population density  $\mathbf{p}_{\text{AUV}}[k]$ . To accomplish this goal, two approaches are presented: *Model Based Control* in which the AUVs follow the estimated fish transition matrix, and *Nonlinear Feedback Control* which attempts to match fish population density directly.

##### A. Control Method 1: Model Based Control

In this first method, to leverage periodic behavior of the fish population, a predetermined number of frequency components  $L$  from the fish transition matrix are used to construct the AUV transition matrix. That is,

$$T_{\text{AUV},ij}[k] = \sum_{x=1}^L \hat{T}_{f,ij}^c[\omega_x] \cos(\omega_x k) + \hat{T}_{f,ij}^s[\omega_x] \sin(\omega_x k) \quad (11)$$

for the coefficients  $\hat{T}_{f,ij}^c$  and  $\hat{T}_{f,ij}^s$  of the Fourier cosine and sine transforms of  $T_{ij}[k]$ , respectively. Generally the frequencies  $\omega_x$  are chosen as the  $L$  frequencies corresponding to the Fourier coefficients of greatest magnitude.

##### B. Control System 2: Nonlinear Feedback Control

In tracking population density, the objective is to minimize the difference between fish population density  $\mathbf{p}_f[k]$  and robot population density  $\mathbf{p}_{\text{AUV}}[k]$ . A feedback control may be used to this end. Defining an error vector  $\mathbf{e}[k] = \mathbf{p}_f[k] - \mathbf{p}_{\text{AUV}}[k]$ , and partition  $V$  into two sets  $V_+$  and  $V_-$ , where  $V_+ = \{i \in V \mid e_i \geq 0\}$  and  $V_- = \{i \in V \mid e_i < 0\}$ . Denote the cardinality of  $V_+$  as  $m$  and the cardinality of  $V_-$  as  $n$ . Then, the following transition matrix  $\mathbf{T}_{\text{AUV}}[k]$  is proposed to incorporate nonlinear feedback control:

$$T_{\text{AUV},ij} = \begin{cases} 1 + mk_j e_j[k] / p_{\text{AUV},j}[k] & i = j \text{ and } j \in V_- \\ 1 & i = j \text{ and } j \in V_+ \\ -k_j e_j[k] / p_{\text{AUV},j}[k] & i \in V_+ \text{ and } j \in V_- \\ 0 & \text{otherwise} \end{cases} \quad (12)$$

where

$$k_j = \min \left\{ \frac{r}{m}, -\frac{p_{\text{AUV}}[k],j}{m e_j[k]} \right\} \quad (13)$$

for some parameter  $0 < r < 1$ . It can be seen that each entry of  $T_{\text{AUV},ij}$  is nonnegative and that each column sums to 1, so that  $\mathbf{T}_{\text{AUV}}[k]$  is a left stochastic matrix.

### C. Proof of Feedback Control Convergence

At time  $k+1$ , the AUV population density error at vertex  $i$  is  $e_i[k+1] = p_{f,i}[k+1] - p_{AUV,i}[k+1]$ . In vector notation:

$$\mathbf{e}[k+1] = \mathbf{p}_f[k+1] - \mathbf{p}_{AUV}[k+1] \quad (14)$$

Assume that  $\mathbf{p}_f[k+1]$  remains constant relative to the faster dynamics of  $\mathbf{p}_{AUV}[k+1]$ , which is a valid assumption considering the AUV velocity relative to the time periods of the periodic fish migrations of interest. Then substitution of (10) into (14) yield for positive errors, where  $i \in V_+$ :

$$\begin{aligned} e_i[k+1] &= p_{f,i}[k] - \left( p_{AUV,i}[k] + \sum_j^n \frac{-k_j e_j[k]}{p_{AUV,j}[k]} p_{AUV,j}[k] \right) \\ &= e_i[k] + \sum_{j \in V_-}^n k_j e_j[k] \end{aligned} \quad (15)$$

And for negative errors, where  $i \in V_-$ :

$$e_i[k+1] = (1 - mk_i) e_i[k] \quad (16)$$

In (16), if  $k_i$  is selected such that  $0 < k_i < 1/m$ , then clearly  $e_i[k] \rightarrow 0$  as  $k \rightarrow \infty$ . Hence all negative errors will decay to 0 over time.

To prove that positive errors will also decay, it can be observed that given a finite number of AUVs, the negative error must balance the positive error. That is, the excess number of AUVs at some vertices with negative error must balance with the deficit number of AUVs at vertices with positive error:

$$\sum_{i \in V_+} e_i[k] = - \sum_{j \in V_-} e_j[k] \quad (17)$$

Since it was shown that all negative errors decay to zero, applying this to (17) yields  $\sum_{i \in V_+} e_i[k] \rightarrow 0$ . Since individual errors  $e_i[k]$  are positive, then for the sum to decay to 0, the individual errors do as well. That is,  $e_i[k] \rightarrow 0$ .

## V. SIMULATION RESULTS AND DISCUSSION

To validate the two control systems' effectiveness for AUV tracking of fish undergoing periodic motion behaviors, both the *model based control* and *nonlinear feedback control* strategies were implemented in a MATLAB simulation and tested against the data set described in Section 1.

A transition model was constructed from one week of location data of a single kelp bass from the Catalina tracks. The fish's behavior during this time was highly periodic, as shown in Fig. 1b. Using this transition model, 100 fish were simulated, and a varying number of AUVs were also simulated. Two sets of simulations were conducted, one where the AUVs employed the model-based controller, and a second where they employed the nonlinear feedback controller. To compare the two control systems, three performance metrics were calculated for each simulation:

- 1) **Closest AUV Distance** The Closest AUV Distance error tracked the distance from each simulated fish to

the closest AUV, averaged across all of the fish and all time steps of the simulation.

- 2) **Population Density Error at Destination Vertex** Population Density Error is a measure between 0 and 1 quantifying the difference between the distribution of simulated fish across the vertices and the distribution of AUVs. For a fish density  $\mathbf{p}_{fish}$  and AUV density  $\mathbf{p}_{AUV}$ , this error is calculated as

$$e = \sqrt{\frac{1}{2} (\mathbf{p}_{fish} - \mathbf{p}_{AUV}) \cdot (\mathbf{p}_{fish} - \mathbf{p}_{AUV})} \quad (18)$$

The Population Density Error at Destination Vertex assumes that the location  $n_{AUV,r}$  of each AUV is its current destination vertex. E.g., as soon as AUV  $r$  transitions from vertex  $i$  to vertex  $j$ , this metric defines  $n_{AUV,r} = j$ .

- 3) **Population Density Error at Closest Vertex** The Population Density Error at Closest Vertex is identical to Population Density Error at Closest Vertex, except the AUV locations are chosen to be the geometrically nearest vertex at each time.

### A. Model Based Control

To simulate the model based control, a transition model using a Gaussian kernel with a smoothing parameter  $h$  of two minutes was fit to 7 days of tracking data from one kelp bass in the data set, whose position was linearly interpolated every two minutes. Since the week of historical data contained 5,040 samples, the resulting transition probability functions contained 2,520 frequency components. The model based control was tested using various numbers of these components, between zero of them for completely random transitions and all of them to have an identical transition matrix to the fish, and with varying numbers of AUVs. A target population of 100 fish following the kelp bass transition model was used in computing the error metrics. The fish and AUVs moved with the same speed, a fair assumption for this species.

Fig. 3a shows the Closest AUV Distance error for each of the combinations of parameters. As would be expected, when more AUVs are present, fish are more likely to be close to an AUV. When 10 or more AUVs are used, i.e., when there are more AUVs than vertices, even random transitions result in an error below 13 meters.

Fig. 3b shows the Population Density Error at Destination Vertex. This error tends to decrease with additional frequency components and is relatively insensitive to the number of AUVs when there are more AUVs than vertices. The errors were overall relatively high, as the model based control passively relies on transition probabilities to match the AUV to fish population density.

Finally, Fig. 3c shows the Population Density Error at Closest Vertex. Larger teams of AUVs and increasing numbers of frequency components used drive this error very close to zero, as the simulated AUVs populations become more similar to the target simulated fish population in size and transition model.

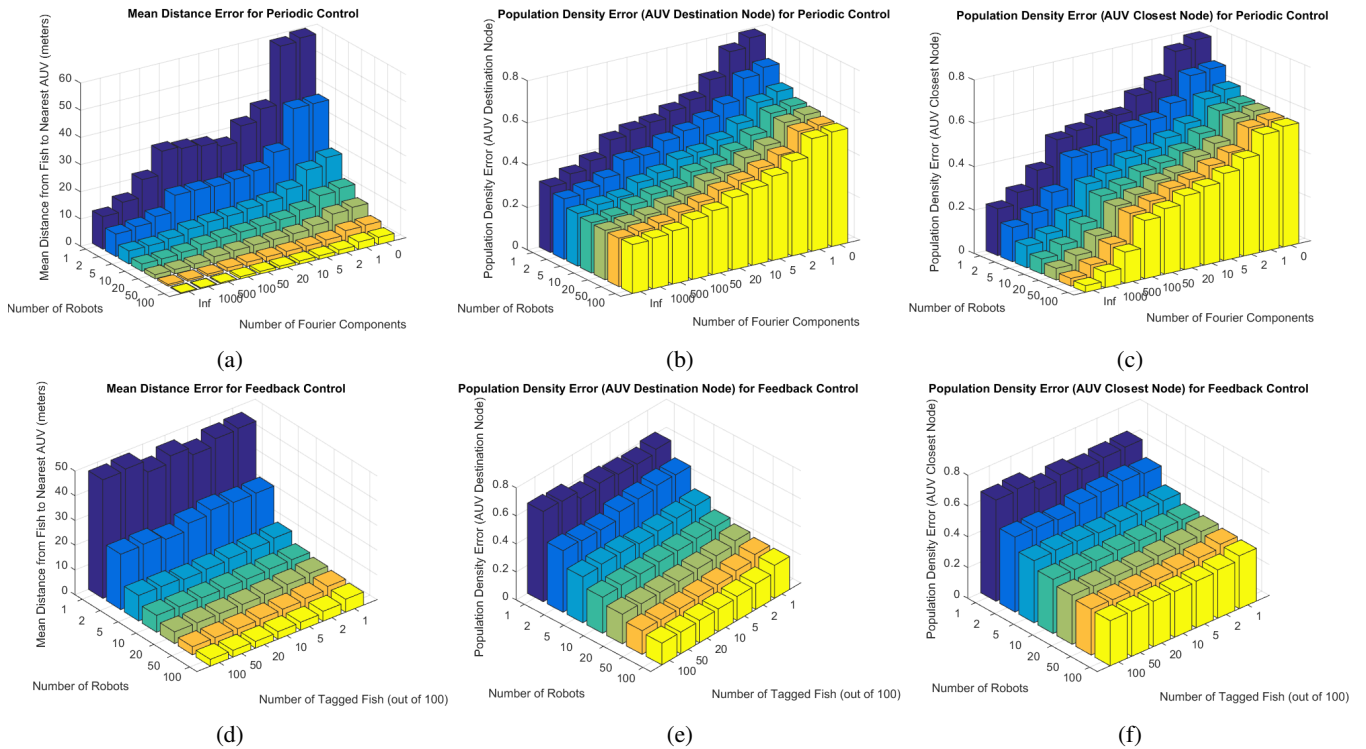


Fig. 3: (a) shows the average distance from a fish to the closest AUV when using the periodic control with varying numbers of AUVs and Fourier components. (b) plots the average population density error metric from (18), where AUV vertex locations are taken to be their current destination; while (c) shows the same error but with AUV vertex locations taken to be the geometrically closest vertex at each time. Plots (d), (e), and (f) show the same error metrics using the feedback control with a gain parameter of  $r = 0.99$  for varying numbers of AUVs and fractions of the population whose locations are known to the controller.

### B. Feedback Control

To simulate the feedback control, the same simulated population of 100 fish following the kelp bass transition model was tracked by AUVs distributed by the feedback control with a gain parameter of  $r = 0.99$  over seven days. Again, AUV teams of various sizes were tested. Additionally, the controller was only made aware of a certain subset of the target population, so that the target AUV population density used by the feedback control to calculate the AUV transition matrix at each time depended on these “tagged” fish. Varying numbers of these “tagged” fish were also tested, between one fish and every fish in the target population. Again, the AUVs and fish moved with the same speed.

Fig. 3d shows the Closest AUV Distance error for these parameters. Since the simulated fish population in these tests follows the transition model of a single fish, the distribution of fish is unimodal; as such, a single tagged fish is usually sufficient to bring the AUVs near most of target population.

Fig. 3e and Fig. 3f show the Population Density Error at Destination Vertex for the feedback control. In both of these plots, error decreased as larger AUV teams allowed the AUV population density to converge on the fish population density to a finer grain. Due to the unimodal distribution of the fish, error depended very little on the number of tagged fish in the population.

These plots show a difference between the performance of the feedback control and the model based control: the model based control had a lower closest-vertex error, while the feedback control had a lower destination vertex error. Due to the feedback control’s active monitoring of the target population density, the feedback control will always direct transitioning AUVs to destination vertices with high fish population densities. But slow AUVs are unable to keep up with rapidly-changing fish densities when they take a long time to transition between vertices, resulting in a higher closest-vertex error. The feedback control in particular benefits from AUVs that are faster than the fish, while the model based control tolerates slower AUV speeds closer to that of the fish.

## VI. FIELD TEST RESULTS AND DISCUSSION

In validating the periodic models and stochastic controller, the system was implemented on an OceanServer Iver2 AUV, (see Fig. 4d). Its actuators include a motor driven propeller and 4 fins to steer. The vehicle has a maximum depth rating of 100m and maximum speed of 4.0 knots. To detect tagged fish, the Lotek hydrophone system is installed on the vehicle. A WHOI Micro-Modem is used for inter-AUV communication. The field trials presented were performed during June, 2015 and December 2015 at Big

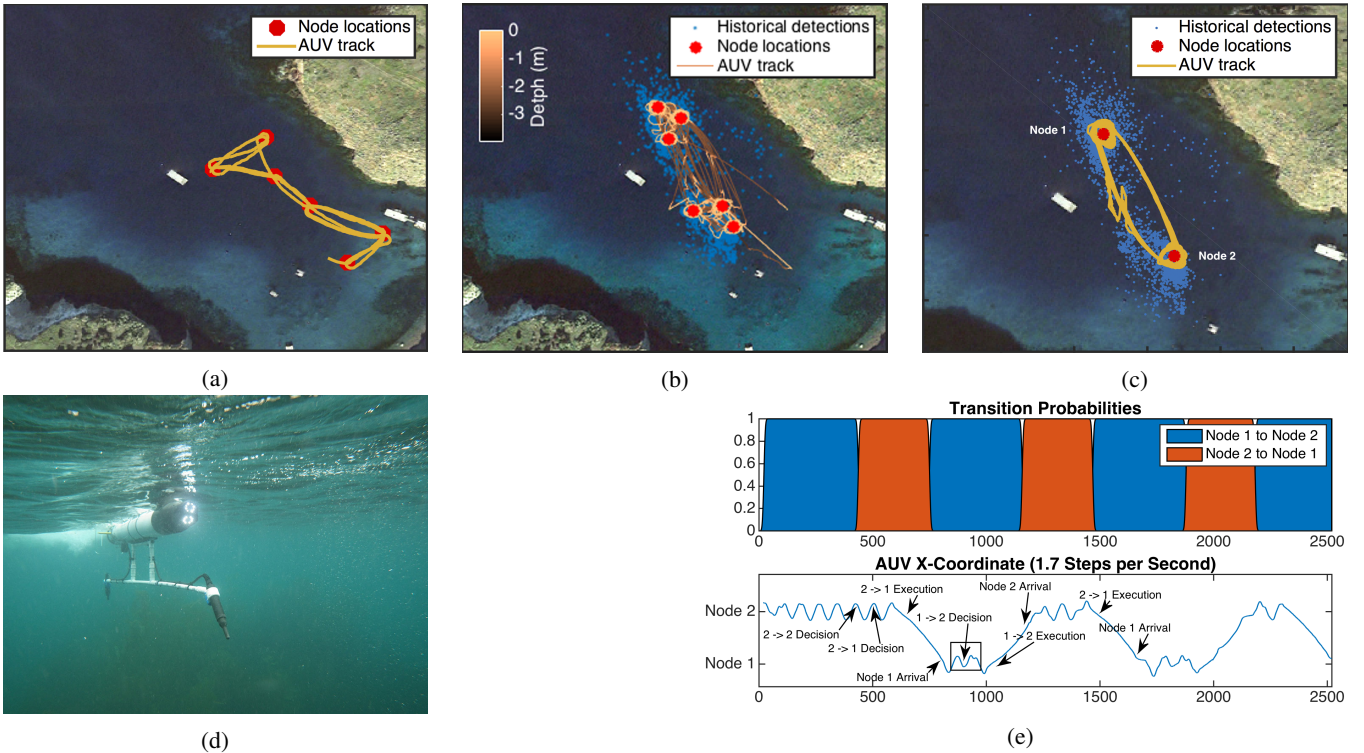


Fig. 4: Results of trial runs shown in (a), (b) and (c). In (a), the six vertex locations are randomly selected. The AUV runs at the surface of the water. In (b), the six vertices are calculated based on the historical fish data. The AUV runs at 0 - 4 meter depth in water. The trial shown in (c) uses the model from historical data set. (d) shows a picture of OceanServer Iver2 AUV that is used for experiments presented in the paper. (e) shows the recorded robot position in relation to the expected transition probabilities for the trial in (c).

Fishermans Cove, Santa Catalina island, California.

#### A. Preliminary System Verification

The results from a system verification trial is shown in Fig. 4a, where the goal was to establish that a real AUV could use a given transition matrix to make stochastic decisions about which vertex to navigate towards, and then autonomously drive to that vertex. The transition matrix was randomly generated for a six vertex graph. The AUV was programmed to transition to a new vertex once it reached within a threshold distance  $\tau$  of vertex  $i$  based on Eq. (19). The experiment lasted for 30 minutes. The AUV successfully transitioned between vertices many times throughout the experiment, demonstrating the ability for the AUV to follow a given transition matrix.

$$|X_{AUV} - X_{node_i}| < \tau \quad (19)$$

#### B. Tracking Historical Fish Detections

For final verification of the system, the transition models and stochastic controller were implemented on the AUV. This included using vertex locations that represented locations from the historical fish detection, as well as a transition model constructed using the method detailed in Section III. To verify the transitions match those of the historical fish data set, two kinds of trials were performed.

First, a two vertex representation of the data set was used as shown in Fig. 4c. This trial shows that the AUV is able to follow the correct transition behavior of the tagged fish during a 24-hour period back and forth between the north and south locations. Since it was infeasible to run a week-long experiment, the experiment was accelerated to fit within a 40-minute window. Unfortunately, accounting for this speedup factor, the AUV moved at a speed a factor of ten slower than that of the fish that generated the historical data set. Consequently, the resulting AUV density did not match well with the target AUV density. Future work should allow more time for experiments to limit the effect of this problem.

The second set of trials were performed using the six vertex representation of the data set, and tests similar to the two-vertex case were performed. The results from Fig. 4c demonstrate the feasibility of implementing the periodic model and stochastic controller onto a physical system, as the data shows the AUV correctly follows the transition probabilities defined by the models.

## VII. CONCLUSIONS AND FUTURE WORK

One graph-based periodic model and two stochastic AUV controllers are presented in the paper. The model based controllers allow a multi-AUV system to track migratory paths of tagged fish groups using data of historical detections. In validation of the controllers, results of simulated and

physical experiments are presented. It is shown that a single AUV system is capable of tracking the transition probabilities of the historical detections based on the models developed in this paper. This work makes several contributions to future fish tracking and interpreting patterns of marine animal movement, including: 1) allowing AUVs to predict where to search for a tagged fish after losing detections, 2) making inferences and predictions of schooling species based on individual historical data, 3), maximizing information gain during monitoring and tracking schools of marine animals, and 4) allowing future development of a multi-AUV system to simultaneous tracking and exploring of a marine environment.

#### ACKNOWLEDGMENT

This material is based upon work supported by the National Science Foundation under Grant No. 1245813. This work was performed in part at the USC Wrigley Institute for Environmental Studies and at the Claremont Colleges Robert J. Bernard Biological Field Station. We would also like to thank Mario Espinoza and Thomas Farrugia for their help tagging fish and maintaining the receiver array to collect data. GPS data rendering was provided by Vemco/Arimix Systems Inc.

#### REFERENCES

- [1] Lowe, C.G. and R.N. Bray. 2006. Fish Movement and Activity Patterns. In: L.G. Allen, M.H. Horn, and D.J. Pondella (eds.). The Ecology of California Marine Fishes. University of California Press: Berkeley, California.
- [2] Lowe, C.G., D.T. Topping, D.P. Cartamil, and Y.P. Papastamatiou. 2003. Movement patterns, home range and habitat utilization of adult kelp bass (*Paralabrax clathratus*) in a temperate no-take marine reserve. *Marine Ecology Progress Series* 256:205-216.
- [3] Teesdale, G.N., B.W. Wolfe, and C.G. Lowe. 2015. Patterns of home ranging, site fidelity, and seasonal spawning migration of barred sand bass caught within the Palos Verdes Shelf Superfund Site. *Marine Ecology Progress Series*. 539:255-269.
- [4] Wolfe, B., C.G. Lowe. 2015. Movement patterns, habitat use and site fidelity of the white croaker (*Genyonemus lineatus*) at the Palos Verdes Super Fund Site, Los Angeles, California. *Marine Environmental Research*. 109:69-80.
- [5] M.R. Heupel, C.A. Simpfendorfer, and R.E. Hueter. Running Before the Storm: Blacktip Sharks Respond to Falling Barometric Pressure Associated with Tropical Storm Gabrielle. *Journal of Fish Biology*, 63(5):13571363, 2003.
- [6] B.V. Hight and C.G. Lowe. Behavioral thermoregulation in adult female leopard sharks, *triakis semifasciata*, in nearshore embayments. *J. of Experimental Marine Biology and Ecology*, 352:114-128, 2007.
- [7] R. Sakabe, and J. M. Lyle. The Influence of Tidal Cycles and Freshwater Inflow on the Distribution and Movement of an Estuarine Resident Fish *Acanthopagrus Butcheri*. *Journal of Fish Biology*, 77, 643-660, 2010.
- [8] B. W. Hartill, M.A. Morrison, M. D. Smith, J. Boube, and D. M. Parsons . Diurnal and Tidal Movements of Snapper (*Pagrus Auratus*, Sparidae) in an Estuarine Environment. *Marine and Freshwater Research* 54 , 931940, 2003.
- [9] A. Acou, P. Laffaille, A. Legault, and E. Feunteun. Migration Pattern of Silver Eel (*Anguilla anguilla*, L.) in an Obstructed River System. *Ecology of Freshwater Fish*, 17, 432-442, 2008.
- [10] K. J. Murchie, S. J. Cooke, A. J. Danylchuk, S. E. Danylchuk, T. L. Goldberg, C. D. Suski, and D. P. Philipp. Movement Patterns of Bonefish (*Albula Vulpes*) in Tidal Creeks and Coastal Waters of Eleuthera, The Bahamas. *Fisheries Research*, 147, 404 - 412, 2013.
- [11] M. Espinoza, T. J. Farrugia, D. M. Webber, F. Smith, and C. G. Lowe. Testing a New Acoustic Telemetry Technique to Quantify Long-Term Finescale Movements of Aquatic Animals. *Fisheries Research*, vol. 108, pp.364371, 2011.
- [12] C. G. Lowe and R. N. Bray, Fish movement and activity patterns, *The Ecology of California Marine Fishes*, pp. 524–553, 2006.
- [13] D. Schulz, W. Burgard, D. Fox, and A. Cramers. Tracking Multiple Moving Objects with a Mobile Robot. in *Computer Vision and Pattern Recognition*, IEEE Computer Society Conference, 2001.
- [14] D. Schulz, W. Burgard, D. Fox, and A. Cremers. People Tracking with Mobile robots Using Sample-Based Joint Probabilistic Data Association Filters. *The International Journal of Robotics Research*, vol. 22, 2003.
- [15] M. Kobilarov, G. Sukhatme, J. Hyams, and P. Batavia. People Tracking and Following with Mobile Robot Using an Omnidirectional Camera and a Laser. in *Proceedings of the 2006 IEEE International Conference on Robotics and Automation*, 2006.
- [16] M. Montemerlo, S. Thrun, and W. Whittaker. Conditional Particle Filters for Simultaneous Mobile Robot Localization and People-Tracking. in *Proceedings of the 2002 IEEE International Conference on Robotics and Automation*, vol. 1, 2002, pp. 695701.
- [17] Y. Lin, H. Kastein, T. Peterson, C. White, C. G. Lowe, and C. M. Clark. Using Time of Flight Distance Calculations for Tagged Shark Localization with an AUV. in *Proceedings of the Unmanned Untethered Submersible Technology Conference*, 2013.
- [18] J. Rife and S. M. Rock. Segmentation Methods for Visual Tracking of Deep-Ocean Jellyfish Using a Conventional Camera. *IEEE Journal of Ocean Engineering*, vol. 28, pp. 595608, 2003.
- [19] J. Zhou and C. M. Clark. Autonomous Fish Tracking by ROV Using Monocular Camera. *Computer and Robot Vision*, Canadian Conference, vol. 0, p. 68, 2006.
- [20] C. Forney, E. Manii, M. Farris, M. Moline, C. G. Lowe, and C. M. Clark. Tracking of a tagged leopard shark with an auv: Sensor calibration and state estimation. in *Proceedings of the 4th International Conference on Robotics and Automation*, 2012.
- [21] N. D. M. Nguyen, K. N. Huynh, N. N. Vo and Tuan Van Pham, Fish detection and movement tracking, *Advanced Technologies for Communications (ATC)*, 2015 International Conference on, Ho Chi Minh City, 2015, pp. 484-489.
- [22] C. M. Clark, C. Forney, E. Manii, D. Shinzaki, C. Gage, M. Farris, C. G. Lowe, and M. Moline. Tracking and Following a Tagged Leopard Shark with an Autonomous Underwater Vehicle. *Journal of Field Robotics*, vol. 30, 2013.
- [23] D. Shinzaki, C. Gage, S. Tang, M. Moline, B. Wolfe, C. G. Lowe, and C. M. Clark. A Multi-AUV System for Cooperative Tracking and Following of Leopard Sharks. in *Proceedings of the IEEE International Conference on Robotics and Automation*, 2013.
- [24] Y. Lin, H. Kastein, T. Peterson, C. White, C. G. Lowe and C. M. Clark, A Multi-AUV State Estimator for Determining the 3D Position of Tagged Fish, *Intelligent Robots and Systems, IEEE/RSJ International Conference on*, Chicago, IL, 2014, pp. 3469-3475.
- [25] T. M. William, M. A. Hsieh, Macroscopic Modeling of Stochastic Deployment Policies with Time Delays for Robot Ensembles. *Int. J. Rob. Res.*, 30, 590-600, 2011.
- [26] S. Berman, A. Halasz, M. A. Hsieh and V. Kumar, Optimized Stochastic Policies for Task Allocation in Swarms of Robots, in *IEEE Transactions on Robotics*, vol. 25, no. 4, pp. 927-937, Aug. 2009.
- [27] S. Berman, A. Halasz, M. A. Hsieh, and V. Kumar, Navigation based Optimization of Stochastic Deployment Strategies for a Robot Swarm to Multiple Sites, in, *Proc. of the 47th IEEE Conference on Decision and Control*, Cancun, Mexico, 2008.
- [28] Lyons, K, E.T. Jarvis, S. Jorgensen, K. Weng, J. OSullivan, C. Winkler, C.G. Lowe. 2013. Assessment of degree and result of fisheries interactions with juvenile white sharks in southern California via fishery independent and dependent methods. *Fisheries Research*. 147:370-380.